Eurasia Specialized Veterinary Publication

International Journal of Veterinary Research and Allied Science
ISSN:3062-357X

2021, Volume 1, Issue 2, Page No: 67-76

Available online at: www.esvpub.com/

Topical Snail Secretion Filtrate Enhances Wound Closure and Tissue Remodeling in Full-Thickness Excisional Wounds in Mice

Ahmed Hassan[1], Fatma Mohamed[1], Mohamed Khaled[1*]

[1]Department of Zoology, Faculty of Science, Menoufia University, Shebin El-Kom, Egypt.

***E-mail** ✉ mohamed.khaled@outlook.com

ABSTRACT

Wound repair is a natural physiological process that proceeds through multiple regulated stages, including inflammation, proliferation, and tissue remodeling. For hundreds of years, Helix aspersa Muller mucus has been recognized for its beneficial biological effects in managing various skin ailments. In this research, a full-thickness excisional wound model in mice was employed to assess whether Snail Secretion Filtrate (SSF) enhances wound repair efficiency. Mucus was extracted from Helix aspersa Muller through gentle mechanical stimulation using a sterile cotton swab and subsequently purified via a series of filtrations to yield SSF. After injury induction, mice received topical SSF treatment daily for 14 days. Macroscopic analysis revealed that SSF markedly accelerated wound closure and increased the percentage of healed tissue area. Moreover, SSF promoted essential wound repair markers such as collagen formation (Masson, COL3A1, and matrix metalloproteinases (MMPs)) and supported tissue remodeling (α-sma, vascular endothelial growth factor (VEGF)). Additionally, SSF mitigated inflammatory activity in damaged tissue (myeloperoxidase (MPO), IL-1β, IL-6, TNF-α). In summary, SSF improved both the rate and quality of wound recovery by modulating several biological phases, particularly the proliferative and remodeling stages.

Keywords: Snail secretion filtrate, Helix aspersa Muller, Wound healing, Matrix metalloproteinases (MMPs)

Received: 14 August 2021
Revised: 18 November 2021
Accepted: 19 November 2021

How to Cite This Article: Hassan A, Mohamed F, Khaled M. Topical Snail Secretion Filtrate Enhances Wound Closure and Tissue Remodeling in Full-Thickness Excisional Wounds in Mice. Int J Vet Res Allied Sci. 2021;1(2):67-76. https://doi.org/10.51847/unDNWKa3Wv

Introduction

The wound healing process is a critical biological mechanism that preserves skin integrity after trauma resulting from external injuries, accidents, or medical interventions. In both animals and humans, this complex process involves sequential phases—namely inflammation, proliferation, and remodeling [1]. When these steps occur properly, full tissue restoration and skin structure recovery are achieved. However, the presence of pathological factors such as infection or chronic disease can interfere with this process, leading to chronic wounds that remain arrested at a specific healing stage [2].

For centuries, the mucus of Helix aspersa Muller has been recognized for its beneficial dermatological effects. Recently, its use has gained renewed attention as an ingredient for cosmeceutical and para-pharmaceutical products aimed at skin repair [1]. This mucus, secreted by epidermal glands covering the snail's body, serves multiple survival functions and possesses adhesive, emollient, antimicrobial [3], and regenerative properties [4, 5]. Despite rising commercial interest, limited scientific evidence exists regarding its precise biological mechanisms and chemical composition, which can vary with species and environmental conditions [5]. The mucus of Helix aspersa Muller contains mucopolysaccharides, hyaluronic acid, polyphenols, and other bioactive molecules and minerals [6]. The mucopolysaccharide content enhances skin adherence, forming a protective

barrier, while polyphenols act against oxidative stress. Moreover, it can stimulate endogenous hyaluronate production, thereby improving the skin's hydration and viscoelasticity [6].

Our previous research examined the properties of crude Snail Secretion Filtrate (SSF). The mucus was manually extracted using sterile cotton swabs and filtered through multiple membranes to obtain a purified sample. In earlier work, we completed the full chemical profiling of SSF and demonstrated its protective activity in a murine model of ethanol-induced gastric ulcers [7]. The filtrate showed high concentrations of mucopolysaccharides, glycolic acid, and collagen, along with allantoin, elastin, vitamins A, B-complex, and E, as well as minerals like copper, nickel, and chromium. Its protective action was linked to the preservation of mucosal mucopolysaccharides and collagen and to reduced oxidative and inflammatory stress [7].

In the current investigation, we assessed SSF's impact on wound healing in a full-thickness excisional mouse model. The study analyzed its influence on molecular and histological parameters, including collagen organization (Masson staining, COL3A1, MMPs), tissue remodeling (VEGF, α-sma, TGF-β), and inflammation (MPO, mast cells, IL-1β, TNF-α).

Materials and Methods

Animals

Male CD1 mice (20–30 g; ENVIGO, Indianapolis, IN, USA) were kept in standard cages (Tecniplast, Italy) under controlled conditions (22 °C, 12 h light/dark cycle) with unrestricted access to food and water. Animals were acclimatized for one week prior to experimentation. The study was approved by the Messina University Animal Care and Use Committee (authorization code 294/2021-PR). All procedures complied with Italian law (D.Lgs 2014/26), EU Directive 2010/63, and ARRIVE guidelines.

Snail secretion filtrate (SSF) preparation and sterilization

Mucus from Helix aspersa Muller was supplied by Snail S.R.L.S (Messina, Italy). The snails were handled under cruelty-free conditions. Mucus was collected through gentle manual stimulation using sterile cotton swabs. Initially, the extract was passed through a coarse filter for pH stabilization, followed by sequential filtration using three membranes (10 µm, 1 µm, and 0.22 µm; Pall). The final filtrate was stored at 4 °C. The 0.22 µm filter step ensured the removal of contaminants and endotoxins, making the product sterile and injectable. A full chemical profile was previously described [7].

Full-thickness excisional wound model

To generate cutaneous wounds, mice were first anesthetized using inhaled isoflurane (3% in air). Dorsal fur was carefully shaved, and the skin was alternately disinfected three times with 70% ethanol and povidone–iodine to ensure sterility. Using a sterile biopsy punch (KAI Corporation, Tokyo, Japan), two round full-thickness wounds, each 5 mm in diameter, were produced symmetrically along both sides of the dorsal midline.

After wounding, animals were randomly allocated to three groups:

- SHAM (n = 10): underwent anesthesia and skin preparation without excision.
- CONTROL (n = 10): received full-thickness excisions followed by topical application of 400 µL sterile distilled water via micropipette once daily for 14 days.
- SSF (n = 10): treated identically, except 400 µL of Snail Secretion Filtrate (SSF) was applied to the wound surface once per day for 14 days.

At designated time points, each wound was photographed under consistent lighting, and the open area was measured with ImageJ software. Wound closure was expressed as a percentage relative to the initial size. On day 14, all mice were humanely euthanized by cervical dislocation under anesthesia. Skin biopsies (10-mm circular samples centered on the wound, containing the full dermal depth) were harvested [8]. The left-side sample was preserved in 4% formaldehyde for microscopic analysis, while the right-side tissue was immediately frozen at −80 °C for biochemical testing.

Histopathological and immunohistochemical evaluation

Collected tissues were fixed in 4% formaldehyde, paraffin-embedded, and sectioned. Hematoxylin–eosin (H&E) staining was performed to examine tissue organization; representative areas encompassing the entire wound bed were viewed at 10× magnification. Tissue regeneration was graded on a 0–4 scale as follows:

0 = >70% of the section lacking epithelial proliferation;
1 = >60% showing disorganized epidermis;
2 = >40% with partial epithelial formation;
3 = >60% displaying moderate epithelial growth;
4 = >80% showing complete remodeling of the epidermis.

Additional 5-µm-thick slices were stained using the Masson trichrome method (Bio-Optica, Italy) to visualize collagen fibers. Blue-stained regions corresponding to collagen were quantified through ImageJ within the wound zone under 10× magnification.
Immunohistochemical staining followed standard protocols. Sections were incubated overnight at 4 °C with primary antibodies: anti-α-sma (Santa Cruz Biotechnology, sc-130617, Heidelberg, Germany), anti-VEGF (1:250; Santa Cruz Biotechnology, sc-57496, Heidelberg, Germany), and anti-MPO (1:250; Santa Cruz Biotechnology, sc-390109, Heidelberg, Germany). Detection procedures were consistent with earlier publications. For each mouse, five stained samples were scored independently by blinded observers using a Leica DM6 microscope (Leica Microsystems SpA, Milan, Italy). Quantification of positive signal intensity in the wound area was expressed as histogram values at 10× and 40× magnifications.

ELISA
The concentration of Collagen Type III Alpha (COL3A1) protein was measured by enzyme-linked immunosorbent assay (ELISA) following the protocol supplied by the manufacturer (Cloud-Clone Corp., Katy, TX, USA).

Toluidine blue staining
For mast cell visualization, paraffin sections were first de-waxed in xylene and rehydrated through graded ethanol baths (5 min per step). Slides were then immersed in distilled water for 5 min, stained with toluidine blue for 4 min, gently blotted, dehydrated in absolute ethanol for 1 min, cleared in xylene, and finally mounted with Eukitt medium (Bio-Optica, Milan, Italy) according to established procedures [9, 10].
Mast cells were enumerated under light microscopy at 40× magnification in five randomly selected fields per sample using a Leica DM6 microscope (Leica, Milan, Italy). These cells were recognized by their metachromatic granules. Elongated or oval cells (10–30 µm) containing dense cytoplasmic granules partially covering a central or eccentric nucleus were counted as mast cells. Fragments of cells or isolated granule deposits were excluded from counts. The results were expressed as mast cell number per unit area of wound bed tissue [11].

Western blot
The Western blot procedure was carried out following earlier methodologies [12–14]. Briefly, membranes were exposed overnight at 4 °C to the following primary antibodies: anti-MMP1 (1:1000; Santa Cruz Biotechnology, sc-137044, Heidelberg, Germany), anti-MMP2 (1:1000; Santa Cruz Biotechnology, sc-13595, Heidelberg, Germany), anti-MMP9 (1:1000; Santa Cruz Biotechnology, sc-393859, Heidelberg, Germany), anti-IL-1β (1:1000; Santa Cruz Biotechnology, sc-52012, Heidelberg, Germany), anti-TGF-β (1:1000; Abcam), and anti-TNF-α (1:1000; Abcam). All antibodies were diluted in 1× PBS supplemented with 5% non-fat dry milk (w/v) and 0.1% TWEEN 20.
After washing, membranes were incubated for 1 h at room temperature with HRP-linked secondary antibodies—either bovine anti-mouse IgG or goat anti-rabbit IgG (1:2000; Jackson ImmunoResearch, West Grove, PA, USA). β-actin (1:2000; Santa Cruz Biotechnology) was used as a housekeeping protein to ensure equal sample loading [15]. Protein detection was achieved using an enhanced chemiluminescence reagent (Bio-Rad, Hercules, CA, USA), and bands were visualized via the Chemi Doc XRS imaging system (Bio-Rad). Quantification of band intensity was performed using Image Lab 3.0 (Bio-Rad), normalizing to the internal control protein. A prestained molecular weight ladder ranging from 10 to 250 kDa (Bio-Rad, Hercules, CA, USA) was employed to estimate molecular weights and verify loading accuracy.

Statistical analysis
Each experiment was repeated three times independently with a sample size of n = 10 per test. All numerical results are presented as mean ± SEM. Differences among datasets were analyzed by an unpaired Student's t-test

or one-way ANOVA followed by Tukey's post hoc test using GraphPad Prism 8 (GraphPad Software Inc., La Jolla, CA, USA). Statistical significance was determined at $p < 0.05$.

Results and Discussion

Acceleration of wound repair by snail secretion filtrate

Figure 1 shows representative images of wounds created with a 5 mm biopsy punch on day 0. To assess the healing capability of SSF, 400 µL of the filtrate was applied daily to the wound area for 14 consecutive days. Based on both wound photographs and closure rate graphs **(Figures 1a and 1b)**, SSF-treated mice exhibited a faster rate of repair and greater percentage reduction of the wound surface between days 3 and 14 compared with untreated controls.

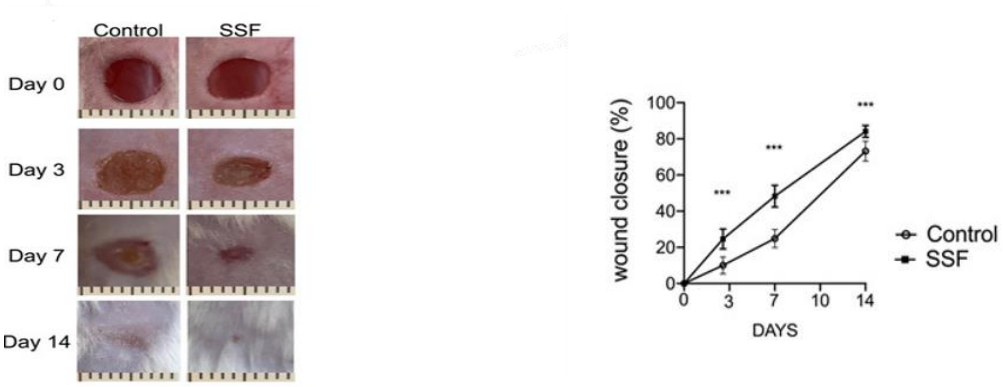

a) b)

Figure 1. Impact of snail secretion filtrate (SSF) on full-thickness wound recovery in mice. (a) Sample wound images at indicated times (scale bar = 1 mm). (b) Percent wound closure over time. Data represent mean ± SEM for 10 animals per group. *** $p < 0.001$ versus control

Influence of SSF on cutaneous healing and collagen reconstruction

As presented in **Figure 2**, histological analysis 14 days after wound creation showed that the control group displayed incomplete epidermal coverage, while topical SSF treatment led to advanced wound repair with improved granulation tissue and nearly full epidermal regeneration. The re-epithelialization score **(Figure 2c)** confirmed a significant elevation in the SSF group relative to controls. Collagen deposition, determined by Masson's trichrome staining, was also enhanced by SSF **(Figure 2b)**, restoring collagen content to a level similar to that seen in sham-treated tissue **(Figure 2d)**. Quantitative measurement of COL3a1 expression **(Figure 2e)** demonstrated a significant increase in COL3a1 levels 14 days following treatment with SSF.

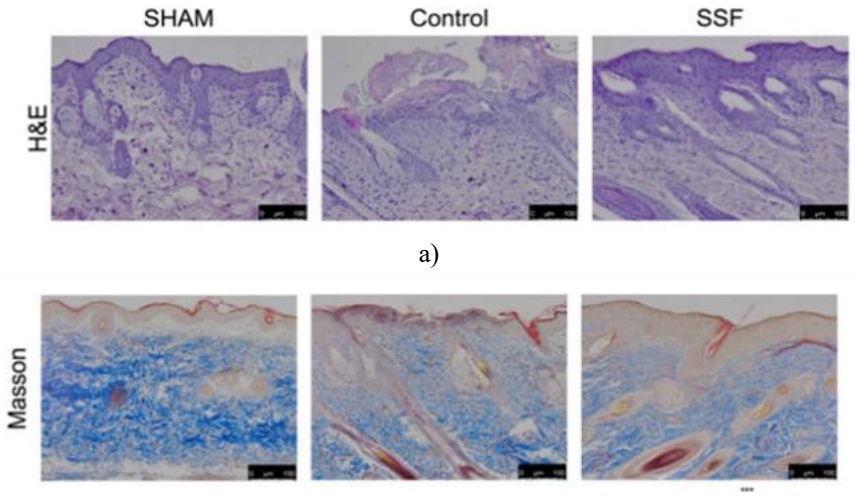

a)

b)

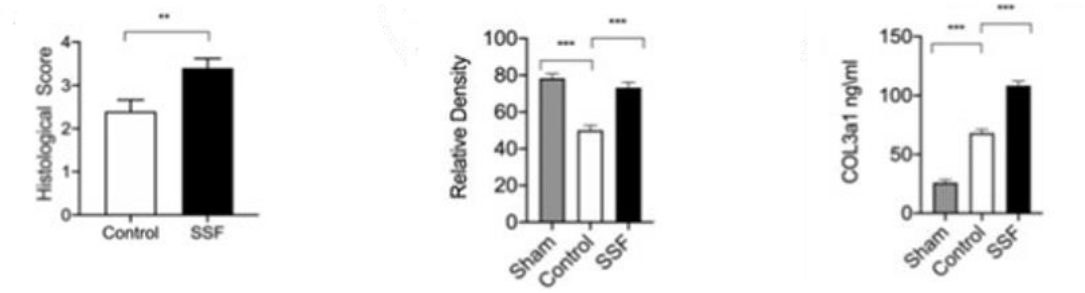

c) d) e)

Figure 2. Influence of SSF on cutaneous wound regeneration and collagen distribution in mice subjected to full-thickness excisional injury. (a,c) H&E-stained sections of granulation tissue collected 14 days after wounding and the corresponding histological scoring chart. (b,d) Assessment of collagen network formation using Masson's trichrome staining on day 14, along with a quantitative plot showing the optical density of the blue-stained collagen fibers. (e) Measurement of COL3a1 levels in wound tissue via ELISA. Values represent mean ± SEM from 10 animals per group. **p < 0.01, ***p < 0.001.

Collagen organization and remodeling are modulated by multiple regulatory molecules, including the metalloproteinase (MMP) enzyme family. To assess their expression, Western blotting was used to detect MMP-1, MMP-2, and MMP-9—key mediators in tissue remodeling during wound recovery. As illustrated in **Figure 3**, SSF treatment prevented the abnormal upregulation of these MMP proteins commonly observed following injury when compared with the untreated control group.

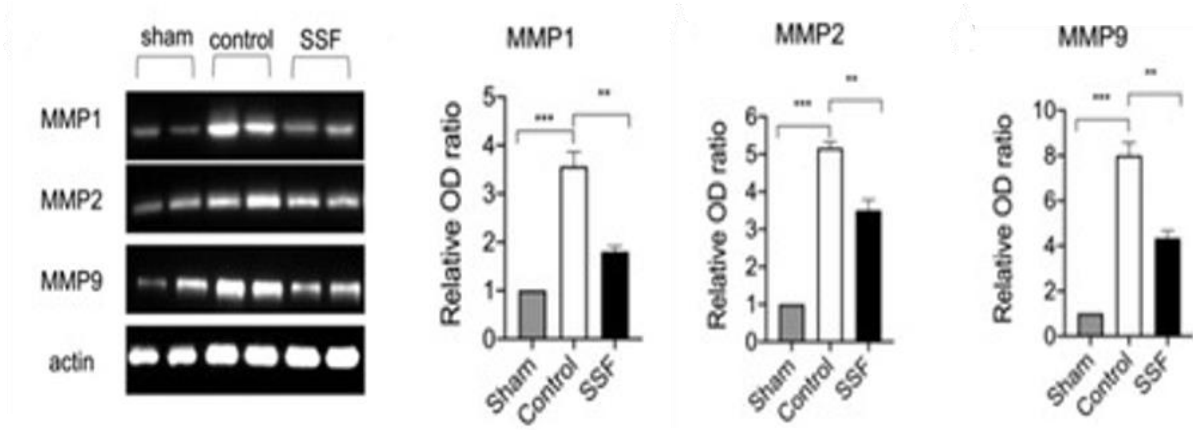

a) b) c) d)

Figure 3. (a) Western blot profiles showing the expression of MMP-1, MMP-2, and MMP-9 in wound tissue, along with their respective densitometric quantifications (b–d). Results are expressed as mean ± SEM for 10 mice per group. **p < 0.01, ***p < 0.001.

SSF modulates α-sma and VEGF expression in wound sites

Immunohistochemical staining was performed to analyze α-sma and VEGF, two critical proteins involved in angiogenesis and tissue differentiation—VEGF being a principal promoter of new vessel formation and α-sma serving as a marker of myofibroblast differentiation. As depicted in **Figure 4**, after 14 days of treatment, the SSF group exhibited markedly enhanced α-sma **(Figures 4a and 4c)** and VEGF **(Figures 4b and 4d)** expression relative to control samples, reflecting improved vascularization and organized tissue architecture.

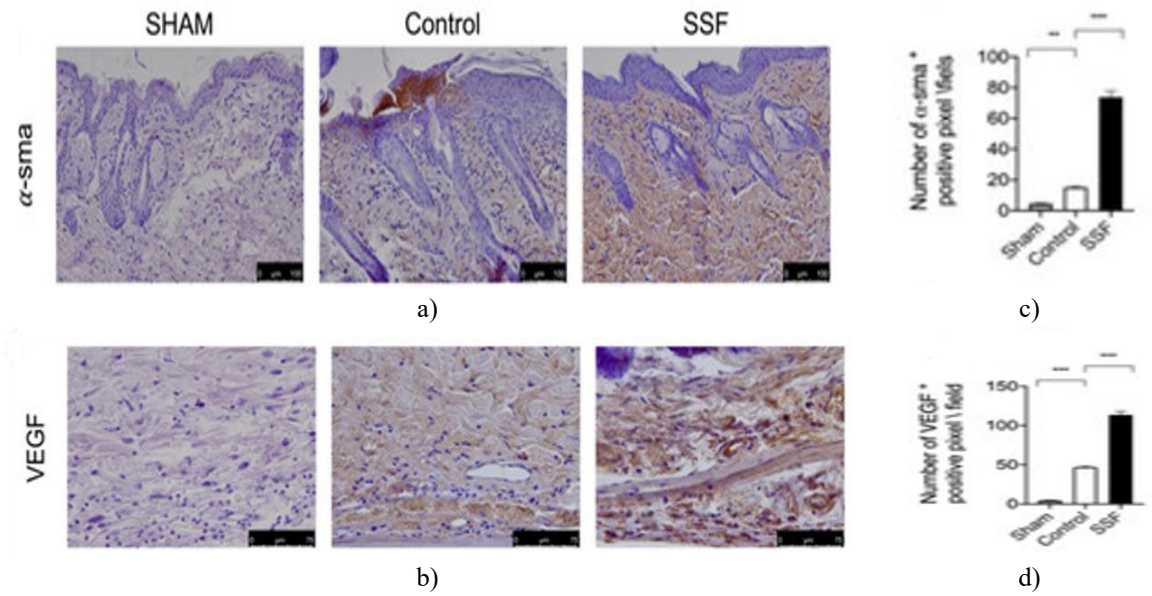

Figure 4. Impact of SSF on α-sma and vascular endothelial growth factor (VEGF) expression in wound tissue. Immunohistochemical visualization of (a,c) α-sma and (b,d) VEGF in wound bed samples. Data are shown as mean ± SEM for 10 animals per group. **p < 0.01, ***p < 0.001.

SSF reduces immune cell Infiltration and attenuates inflammation

Since the inflammatory phase is fundamental in tissue regeneration, we next examined immune cell recruitment by detecting myeloperoxidase (MPO)-positive cells. As seen in **Figures 5a and 5c**, control animals exhibited a higher number of MPO+ cells relative to the sham group, while mice receiving SSF for 14 consecutive days displayed a notable reduction in MPO expression within wound sites. Furthermore, toluidine blue staining was applied to identify mast cells, another immune component crucial for skin balance. Images and quantifications in **Figures 5b and 5d** revealed an elevated mast cell density in the untreated control wounds compared with sham tissue, whereas daily SSF treatment significantly decreased their numbers.

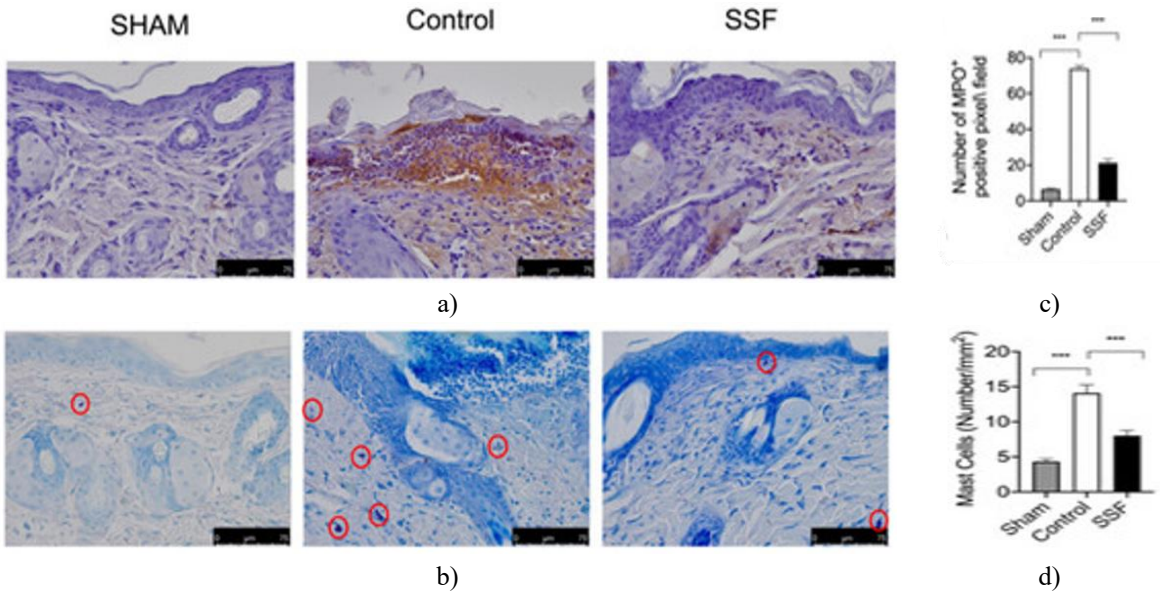

Figure 5. (a,c) Immunohistochemical staining for MPO in sham, control, and SSF-treated wounds 14 days post-injury. SSF administration led to a clear decrease in MPO labeling. (b,d) Mast cell visualization using toluidine blue staining in the same groups. Data expressed as mean ± SEM for 10 mice per group. ***p < 0.001.

Neutrophils and mast cells both participate in the early inflammatory response. Mast cells, in particular, secrete numerous bioactive compounds such as cytokines and growth mediators. Cytokine profiling of wound tissue

indicated that 14 days after injury, control animals showed pronounced overexpression of the pro-inflammatory cytokines IL-1β and TNF-α **(Figures 6a, 6b and 6d)**. Topical administration of SSF effectively suppressed these elevations. In addition, as shown in **Figures 6a and 6c**, SSF restored TGF-β levels, a growth factor associated with tissue remodeling, toward values seen in uninjured skin.

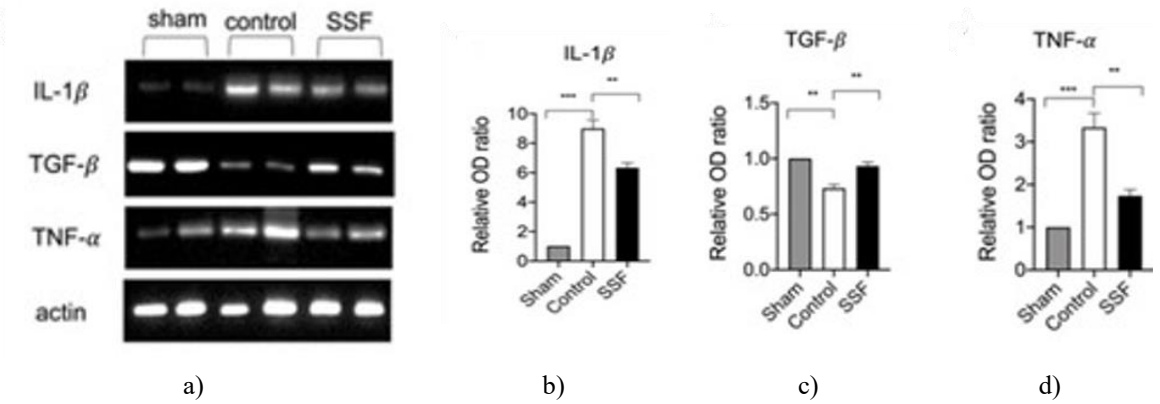

Figure 6. (a) Western blot analyses of wound tissue detecting (b) IL-1β, (c) TGF-β, and (d) TNF-α, along with their corresponding densitometric data. Values are mean ± SEM from 10 mice in each experimental group. **p < 0.01, ***p < 0.001.

Discussion

Skin damage is a widespread condition that may arise from numerous external and internal causes. The restoration of injured skin is a complex biological phenomenon that unfolds through four dynamic and overlapping stages: hemostasis, inflammation, proliferation, and tissue remodeling or resolution [16, 17].

Continuous scientific effort is devoted to identifying novel compounds and strategies that can accelerate and enhance tissue repair. Among these, the therapeutic use of snail mucus has been recognized for centuries in folk medicine; however, detailed knowledge regarding its chemical profile and molecular mechanisms of action remains limited. Formulations derived from snail secretion have recently gained notable interest in dermatological and cosmetic applications because of their hydrating, soothing, protective, and regenerative features [18]. *Helix aspersa* Müller, in particular, produces a distinctive secretion rich in biologically active molecules, whose skin-protective attributes are linked to its mucopolysaccharide matrix and physicochemical characteristics [6].

In our earlier research, we demonstrated that Snail Secretion Filtrate (SSF) exerted a gastroprotective effect in a murine model of ethanol-induced gastric ulcer and provided its chemical composition [7]. We found that SSF contains abundant mucopolysaccharides, high concentrations of glycolic acid and collagen, and notable levels of allantoin and elastin, as well as vitamins A, B-complex, and E, along with trace minerals such as copper, nickel, and chromium. While each of these elements individually supports tissue repair, previous findings indicated that the synergistic composition of whole mucus offers a more potent biological response than isolated constituents [1].

In the present work, we employed a full-thickness excisional wound model in mice to evaluate whether SSF could accelerate dermal healing. Mice received topical SSF for 14 days following injury. Macroscopic observations revealed that animals treated with SSF displayed a faster closure rate and greater percentage reduction in wound area than untreated controls. Histologically, 14 days post-wounding, SSF-treated mice exhibited a well-organized wound bed structure with more advanced epithelial regeneration compared with controls.

Collagen is fundamental in tissue repair, functioning as a major component of the extracellular matrix and contributing throughout all phases of healing [19]. Its regulated synthesis, deposition, and maturation are essential for proper recovery [20]. To visualize collagen organization, we applied Masson's trichrome staining, which revealed markedly enhanced collagen accumulation in SSF-treated wounds relative to controls. Moreover, ELISA quantification showed a significant elevation of COL3A1 (collagen α-1 type III)—a collagen subtype abundant in elastic connective tissues such as skin, lungs, and blood vessels—indicating improved collagen synthesis and maturation in SSF-treated samples [21].

These findings collectively support the conclusion that SSF exerts strong pro-healing effects by promoting collagen production and structural restoration. Collagen metabolism is tightly regulated by matrix

metalloproteinases (MMPs), enzymes that remodel the extracellular matrix during all stages of repair [22, 23]. Dysregulated expression of MMP-1, MMP-2, or MMP-9 can delay epithelial renewal and proper remodeling [24]. Our data demonstrated that SSF normalized the expression of these MMPs, helping maintain a balanced extracellular matrix and thereby supporting tissue reconstruction.

All these coordinated effects contribute to the development of healthy granulation tissue, an essential component for successful wound closure. Adequate granulation tissue ensures vascularization and wound contraction—two processes central to efficient repair [25].

Formation of such tissue relies on the presence of myofibroblasts, specialized cells capable of contracting granulation tissue and narrowing wound margins [26]. For this reason, we investigated the expression of VEGF, a critical regulator of angiogenesis, and α-sma, a marker of myofibroblast differentiation [27]. SSF treatment significantly enhanced both VEGF and α-sma expression levels, indicating improved neovascularization and fibroblast-to-myofibroblast transition, which likely explain the accelerated wound closure observed.

Although wound-healing dynamics differ among species, earlier reports have shown that in rodents, wound contraction mainly occurs after epithelial restoration. Thus, the simple excisional wound model in mice provides a clear and reproducible platform to assess re-epithelialization and evaluate the healing process in a controlled manner [28].

The inflammatory response that follows an injury represents a key biological defense mechanism. During the initial stage after tissue damage, immune activation occurs, initiating localized inflammation accompanied by the recruitment of defense cells. Nevertheless, if this reaction becomes prolonged or excessive, it can interfere with normal repair mechanisms [29]. Although immune activity is vital at the beginning of the recovery process, its sustained overactivation is known to hinder tissue regeneration [29].

In this experiment, the control group exhibited a notable accumulation of mast cells—identified by toluidine blue staining—and leukocytes, recognized as MPO-positive cells, even 14 days after the wound was created. Under the microscope, mast cells were recognized by their distinctive metachromatic granules, but the toluidine blue technique has certain drawbacks [30], such as a lower staining yield compared with other histological methods [31].

Treatment with SSF significantly lessened immune cell infiltration in the damaged area compared with untreated controls, though it did not fully prevent immune cell migration, which still exceeded that in the sham group. Mast cells release numerous bioactive compounds, including cytokines and growth mediators [32]. For this reason, the expression of IL-1β, TNF-α, and TGF-β was analyzed in the wound tissues 14 days after the injury. Prolonged and elevated levels of pro-inflammatory cytokines over an extended period are known to delay wound progression by preventing the shift from inflammation to proliferation [33]. Conversely, growth mediators such as TGF-β are indispensable in coordinating tissue repair by modulating inflammation, stimulating keratinocyte growth and movement, encouraging new vessel formation, supporting collagen synthesis, and remodeling the extracellular matrix [34]. Insufficient levels of TGF-β have been associated with poor recovery outcomes [35].

The findings demonstrated that SSF treatment markedly suppressed the expression of IL-1β and TNF-α, aligning with the observed reduction in immune infiltration. Furthermore, SSF application enhanced the expression of TGF-β, suggesting that it promotes a more balanced and efficient healing process.

Conclusion

Overall, the outcomes of this research indicated that SSF treatment accelerated the overall rate of tissue restoration. SSF appeared to beneficially influence key stages of recovery, particularly those involving inflammation and proliferation. Given the compound's complex chemical composition, it is likely that the biological activity arises from the combined interaction of multiple components rather than a single molecule. As such, its therapeutic potential should be considered as an integrated effect. Collectively, these observations propose that SSF could serve as a promising agent for managing wounds in both clinical and veterinary contexts.

Acknowledgments: None

Conflict of Interest: None

Financial Support: None

Ethics Statement: None

References

1. Tsoutsos D, Kakagia D, Tamparopoulos K. The efficacy of Helix aspersa Muller extract in the healing of partial thickness burns: a novel treatment for open burn management protocols. J Dermatol Treat. 2009;20(4):219-22.
2. Ellijimi C, Ben Hammouda M, Othman H, Moslah W, Jebali J, Mabrouk HB, et al. Helix aspersa maxima mucus exhibits antimelanogenic and antitumoral effects against melanoma cells. Biomed Pharmacother. 2018;101:871-80.
3. Pitt SJ, Graham MA, Dedi CG, Taylor-Harris PM, Gunn A. Antimicrobial properties of mucus from the brown garden snail Helix aspersa. Br J Biomed Sci. 2015;72(4):174-81.
4. Trapella C, Rizzo R, Gallo S, Alogna A, Bortolotti D, Casciano F, et al. HelixComplex snail mucus exhibits pro-survival, proliferative and pro-migration effects on mammalian fibroblasts. Sci Rep. 2018;8:17665.
5. Greistorfer S, Klepal W, Cyran N, Gugumuck A, Rudoll L, Suppan J, et al. Snail mucus—glandular origin and composition in Helix pomatia. Zoology (Jena). 2017;122:126-38.
6. Gentili V, Bortolotti D, Benedusi M, Alogna A, Fantinati A, Guiotto A, et al. HelixComplex snail mucus as a potential technology against O3 induced skin damage. PLoS ONE. 2020;15(2):e0229613.
7. Gugliandolo E, Cordaro M, Fusco R, Peritore AF, Siracusa R, Genovese T, et al. Protective effect of snail secretion filtrate against ethanol-induced gastric ulcer in mice. Sci Rep. 2021;11:3638.
8. Hu C, Chu C, Liu L, Wang C, Jin S, Yang R, et al. Dissecting the microenvironment around biosynthetic scaffolds in murine skin wound healing. Sci Adv. 2021;7(21).
9. Impellizzeri D, Di Paola R, Cordaro M, Gugliandolo E, Casili G, Morittu VM, et al. Adelmidrol, a palmitoylethanolamide analogue, as a new pharmacological treatment for the management of acute and chronic inflammation. Biochem Pharmacol. 2016;119:27-41.
10. Di Paola R, Fusco R, Gugliandolo E, D'Amico R, Campolo M, Latteri S, et al. The antioxidant activity of pistachios reduces cardiac tissue injury of acute ischemia/reperfusion (I/R) in diabetic streptozotocin (STZ)-induced hyperglycaemic rats. Front Pharmacol. 2018;9:51.
11. Liu DR, Xu XJ, Yao SK. Increased intestinal mucosal leptin levels in patients with diarrhea-predominant irritable bowel syndrome. World J Gastroenterol. 2018;24(1):46-57.
12. Esposito E, Impellizzeri D, Bruschetta G, Cordaro M, Siracusa R, Gugliandolo E, et al. A new co-micronized composite containing palmitoylethanolamide and polydatin shows superior oral efficacy compared to their association in a rat paw model of carrageenan-induced inflammation. Eur J Pharmacol. 2016;782:107-18.
13. Irrera N, Arcoraci V, Mannino F, Vermiglio G, Pallio G, Minutoli L, et al. Activation of A2A receptor by PDRN reduces neuronal damage and stimulates WNT/beta-CATENIN driven neurogenesis in spinal cord injury. Front Pharmacol. 2018;9:506.
14. Pallio G, Micali A, Benvenga S, Antonelli A, Marini HR, Puzzolo D, et al. Myo-inositol in the protection from cadmium-induced toxicity in mice kidney: an emerging nutraceutical challenge. Food Chem Toxicol. 2019;132:110675.
15. Cordaro M, Siracusa R, Impellizzeri D, D'Amico R, Peritore AF, Crupi R, et al. Safety and efficacy of a new micronized formulation of the ALIAmide palmitoylglucosamine in preclinical models of inflammation and osteoarthritis pain. Arthritis Res Ther. 2019;21:254.
16. Gosain A, DiPietro LA. Aging and wound healing. World J Surg. 2004;28(3):321-6.
17. Takeo M, Lee W, Ito M. Wound healing and skin regeneration. Cold Spring Harb Perspect Med. 2015;5(1):a023267.
18. Lopez Angulo DE, do Amaral Sobral PJ. Characterization of gelatin/chitosan scaffold blended with aloe vera and snail mucus for biomedical purpose. Int J Biol Macromol. 2016;92:645-53.
19. Fleck CA, Simman R. Modern collagen wound dressings: function and purpose. J Am Coll Certif Wound Spec. 2010;2(3):50-4.
20. Upadhyay A, Chattopadhyay P, Goyary D, Mitra Mazumder P, Veer V. Ixora coccinea enhances cutaneous wound healing by upregulating the expression of collagen and basic fibroblast growth factor. ISRN Pharmacol. 2014;2014:751824.

21. Upadhyay A, Chattopadhyay P, Goyary D, Mazumder PM, Veer V. Eleutherine indica L. accelerates in vivo cutaneous wound healing by stimulating Smad-mediated collagen production. J Ethnopharmacol. 2013;146(2):490-4.
22. Yager DR, Nwomeh BC. The proteolytic environment of chronic wounds. Wound Repair Regen. 1999;7(6):433-41.
23. Fray MJ, Dickinson RP, Huggins JP, Occleston NL. A potent, selective inhibitor of matrix metalloproteinase-3 for the topical treatment of chronic dermal ulcers. J Med Chem. 2003;46(16):3514-25.
24. Mulholland B, Tuft SJ, Khaw PT. Matrix metalloproteinase distribution during early corneal wound healing. Eye (Lond). 2005;19(5):584-8.
25. Bonte F, Dumas M, Chaudagne C, Meybeck A. Influence of asiatic acid, madecassic acid, and asiaticoside on human collagen I synthesis. Planta Med. 1994;60(2):133-5.
26. Xu R, Xia H, He W, Li Z, Zhao J, Liu B, et al. Controlled water vapor transmission rate promotes wound-healing via wound re-epithelialization and contraction enhancement. Sci Rep. 2016;6:24596.
27. Nissen NN, Polverini PJ, Koch AE, Volin MV, Gamelli RL, DiPietro LA. Vascular endothelial growth factor mediates angiogenic activity during the proliferative phase of wound healing. Am J Pathol. 1998;152(6):1445-52.
28. Chen L, Mirza R, Kwon Y, DiPietro LA, Koh TJ. The murine excisional wound model: contraction revisited. Wound Repair Regen. 2015;23(6):874-7.
29. Koh TJ, DiPietro LA. Inflammation and wound healing: the role of the macrophage. Expert Rev Mol Med. 2011;13:e23.
30. Mayhew TM. The new stereological methods for interpreting functional morphology from slices of cells and organs. Exp Physiol. 1991;76(5):639-65.
31. Damsgaard TE, Olesen AB, Sorensen FB, Thestrup-Pedersen K, Schiotz PO. Mast cells and atopic dermatitis. Stereological quantification of mast cells in atopic dermatitis and normal human skin. Arch Dermatol Res. 1997;289(5):256-60.
32. Mukai K, Tsai M, Saito H, Galli SJ. Mast cells as sources of cytokines, chemokines, and growth factors. Immunol Rev. 2018;282(1):121-50.
33. Landen NX, Li D, Stahle M. Transition from inflammation to proliferation: a critical step during wound healing. Cell Mol Life Sci. 2016;73(20):3861-85.
34. Schultz GS, Wysocki A. Interactions between extracellular matrix and growth factors in wound healing. Wound Repair Regen. 2009;17(2):153-62.
35. Blakytny R, Jude E. The molecular biology of chronic wounds and delayed healing in diabetes. Diabet Med. 2006;23(6):594-608.